Evaluating the Efficacy and Minimum Effective Dosage of Mesenchymal Stem Cell Therapy in a Murine Model of Critical Limb Ischemia

Do Jung Kim

The Graduate School
Yonsei University
Department of Medicine

Evaluating the Efficacy and Minimum Effective Dosage of Mesenchymal Stem Cell Therapy in a Murine Model of Critical Limb Ischemia

A Dissertation Submitted
to the Department of Medicine
and the Graduate School of Yonsei University
in partial fulfillment of the
requirements for the degree of
Doctor of Philosophy in Medical Science

Do Jung Kim

June 2024

**This certifies that the Dissertation
of Do Jung Kim is approved.**

Thesis Supervisor Young-Nam Youn

Thesis Committee Member Jae Kwang Shim

Thesis Committee Member Sang-Hyun Lim

Thesis Committee Member Jung-Sun Kim

Thesis Committee Member Chul Hoon Kim

**The Graduate School
Yonsei University
June 2024**

ACKNOWLEDGEMENTS

I thank all my senior professors, colleagues, juniors, and family members who supported and guided me in my journey from becoming a doctor to a cardiovascular surgeon.

I express my sincere gratitude to my advisor, Professor Young-Nam Youn, for his unwavering support, invaluable guidance, and insightful feedback throughout this research. I am also grateful to the members of my research committee (Professor Jae Kwang Sim, Professor Sang-Hyun Lim, Professor Jung Sun Kim, and Professor Chul Hoon Kim) for their valuable input and constructive criticism.

Most importantly, I would like to express my gratitude and love to my family and friends who have supported and loved me.

TABLE OF CONTENTS

LIST OF FIGURES

LIST OF TABLES

ABSTRACT

Evaluating the Efficacy and Minimum Effective Dosage of Mesenchymal Stem Cell Therapy in a Murine Model of Critical Limb Ischemia

Purpose: This study aimed to investigate the therapeutic potential of embryonic stem cell-derived mesenchymal stem cells (E-MSCs) in mitigating tissue damage and promoting angiogenesis under ischemic conditions, such as critical limb-threatening ischemia. Additionally, we aimed to determine the optimal dose required to achieve effective treatment outcomes.

Material and Methods: A hindlimb ischemia model was established using 85 BALB/c nude mice (7-week-old, female). The mice were divided into five groups of 17 mice each: non-ischemia (Group 1, sham), saline-treated ischemia (Group 2, control), and E-MSC-treated ischemia using low, medium, and high doses of treatment (Groups 3–5). The efficacy and minimum effective dosage were evaluated using the rotarod test, necrosis assays, blood perfusion ratio; and histological, inflammatory, and angiogenic cytokine analyses.

Results: Laser Doppler perfusion imaging showed significant recovery in blood perfusion ratios in E-MSC-treated groups compared to controls, with the medium-dose group showing the most notable improvement. In the E-MSC-treated groups, motor function improved over time; however, no significant difference was noted in the necrosis score among groups. The expression of inflammatory cytokines (tumor necrosis factor-α, interleukin (IL)-1β, IL-6, and transforming growth factor-β) and angiogenic cytokines (angiopoietin-1, fibroblast growth factor, vascular endothelial growth factor, and platelet-derived growth factor) increased in the ischemia-induced groups. In the E-MSC-treated groups, initial inflammatory cytokine expression decreased, whereas angiogenic cytokine expression increased compared to Group 2. However, no significant differences were found based on the dose of E-MSCs. Ischemia-induced groups showed decreased myofiber thickness and number, increased inflammatory cells, and collagen fibers compared to sham. Over time, E-MSC-treated groups showed similar myofiber thickness but increased myofiber number and decreased inflammatory cells and collagen fibers compared to controls, with no dose-dependent differences.

Conclusion: While E-MSCs enhanced blood perfusion and regulated cytokines in the ischemic hindlimb model, dose-related differences were not significant. These cells exhibit crucial pro-angiogenic and immunomodulatory effects necessary for tissue repair. However, further research is needed to determine the optimal dose that maximizes their efficacy and to gain a precise understanding of the mechanisms for clinical application.

Key words: embryonic stem cell-derived mesenchymal stem cell, neovascularization, immune modulation, peripheral arterial disease, critical limb ischemia

1. INTRODUCTION

Critical limb-threatening ischemia (CLTI) is a severe vascular disorder characterized by extremely insufficient blood flow, which causes tissue damage and impairs limb function[1,2]. Most patients with CLTI present with comorbidities such as diabetes and other concomitant vascular diseases, because of which they are unsuitable for surgical interventions[3,4]. Even in cases where surgical intervention is feasible, challenges such as poor conduit vessels for bypass or inadequate patency of the proximal arteries frequently result in suboptimal surgical outcomes[5]. Furthermore, endovascular interventions using angioplasty and stenting have shown limited success in reducing limb amputation and mortality rates owing to high rates of restenosis[6]. Despite advances in medical treatment and revascularization procedures, current treatment options for CLTI have significant limitations; innovative approaches are urgently required to enhance tissue repair and promote neovascularization.

Mesenchymal stem cells (MSCs) have emerged as a promising therapeutic tool in regenerative medicine because of their unique characteristics, including self-renewal, immunomodulatory properties, multilineage differentiation potential, and secretion of pro-angiogenic factors[7,8]. Hence, MSCs are potential candidates for treating various degenerative and ischemic conditions, including CLTI, myocardial infarction, and stroke[9-11]. Among the diverse sources of MSCs, embryonic stem cell-derived mesenchymal stem cells (E-MSCs) have emerged as promising candidates for cell-based therapy[11-13]. E-MSCs offer distinct advantages owing to their pluripotent nature and differentiability into cells of all three germ layers. Moreover, E-MSCs exhibit a remarkable capacity for high proliferation and expansion, enabling rapid growth in culture and stable immunomodulatory properties; hence, they are potential candidates for efficient regenerative therapies[14,15].

We have previously demonstrated the potential of adipose-derived MSCs to enhance angiogenesis in a rat hindlimb ischemia model[16]. However, considering the significance of cell dosage in human clinical trials, experiments at various concentrations are necessary[17]. Establishing the efficacy of MSCs and determining their minimum effective dosage could provide a substantive impetus for advancing clinical trials in patients with CLTI. Therefore, this study aimed to investigate the therapeutic effects of E-MSCs on angiogenesis and inflammatory modulation in a murine model of hindlimb ischemia, which mimics CLTI. Additionally, we examined variations in response to various dosages of E-MSCs.

2. MATERIALS AND METHODS

2.1. Animals

All experiments were conducted in accordance with the guidelines approved by the Institutional Animal Care and Use Committee (IACUC) of the Nonclinical Research Institute, CORESTEMCEMON Inc. (Serial No.: 2023-0523) to ensure ethical treatment of the animals throughout the study. BALB/c nude mice are used in critical limb ischemia models owing to their

immunodeficiency, which allows for transplantation without immune rejection, enhances engraftment of transplanted cells, and ensures standardized experimental conditions. A total of 85 BALB/c nude mice (7-week-old, female, weighing 17.6 ± 0.9 g) were raised under standard conditions (22 ± 3 °C; 12-h light/dark cycle, 55 ± 15% humidity, 150–300 luminous intensity). Based on the experimental conditions, the mice were categorized into two main groups: non-ischemic group (n = 17) and ischemic group (n = 68).

In the non-ischemic group, unilateral limb ischemia was not induced; this group was designated as the sham group (n = 17, Group 1). Conversely, the ischemia group (n = 68) was further divided into four subgroups (Groups 2, 3, 4, and 5) based on the E-MSC concentration used in the intramuscular injections:

- Group 2 (n = 17) was treated with saline and designated as the control group.
- Group 3 (n = 17) was treated with a low E-MSC dose (2.5×10^6 cells/kg).
- Group 4 (n = 17) was treated with a medium E-MSC dose (5.0×10^6 cells/kg).
- Group 5 (n = 17) was treated with a high E-MSC dose (7.5×10^6 cells/kg).

2.2. Isolation and culture of E-MSCs

Human E-MSCs were obtained from Daewoong Pharmaceutical Co. Ltd. (Seoul, South Korea)[18]. E-MSCs were cultured in a StemPro MSC SFM XenoFree medium (Gibco, Waltham, MA, USA) supplemented with 1% L-glutamine (Gibco) on Corning CellBIND surface cell culture plates (Corning Inc., Corning, NY, USA) at 37°C. Upon reaching 80–90% confluence, the E-MSCs were subcultured thrice and cryopreserved in liquid nitrogen. E-MSCs were characterized using the modified minimal criteria for MSCs according to the International Society for Cellular Therapy[19]. The E-MSC yield was evaluated by counting total and live nucleated cells using an automated cell counter (Cedex HiRes Analyzer, Roche, Basel, Switzerland). Cell viability was calculated as the percentage of live cells relative to the total cell count. Cell surface markers were analyzed via flow cytometry using a FACSLyric flow cytometer (BD Biosciences, Franklin Lakes, NJ, USA) and FACSuite software (BD Biosciences).

2.3. Hindlimb ischemic model

Prior to the experiment, all animals were thoroughly examined for any abnormalities, and their body weights were recorded. Subsequently, 85 mice with body weights closest to the mean were randomly selected and assigned to each group to ensure an even distribution of average body weights.

After acclimation for 8 days, mice were anesthetized using 3% isoflurane inhalation for respiratory anesthesia. The skin of the left hindlimb was disinfected using 70% ethanol. To establish a hindlimb ischemia model, a skin incision was performed to expose the left iliac and femoral arteries. The femoral artery, vein, and nerve bundles were separated from the muscle tissue. Subsequently, the femoral, proximal caudal femoral, and superficial caudal epigastric arteries were cauterized with a Bovie and then excised[20], effectively creating an ischemic condition in the left hindlimb (Figure 1). The skin was sutured using 6–0 silk sutures**.** The right hindlimb was used as a control. After 1–2 h, saline, and different E-MSC doses were injected directly into the abductor muscle at three points

around the incision site.

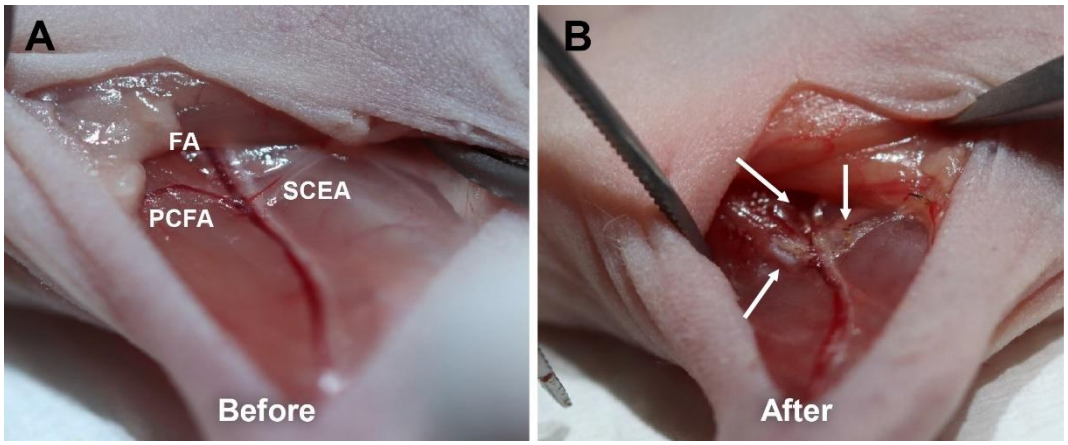

Figure 1. Induction of hindlimb ischemia in a mouse. (A) Before ischemia induction: Exposure of arteries after skin incision of the left hindlimb in a mouse. (B) After ischemia induction: White arrows indicate cauterized and incised arteries.
FA, femoral artery; PCFA, proximal caudal femoral artery; SCEA, superficial caudal epigastric artery

2.4. The rotarod test

The rotarod test was performed before the experiment and 1, 3, 7, 14, and 21 days post-surgery to evaluate motor function and balance in experimental mice. The tests were conducted using a rotarod apparatus, consisting of a rotating rod with an adjustable speed and a timer to record the time for which the mice remained on the rod[21]. The animals were pre-trained on the rotarod for 3 days before the first measurement. On the testing day, each mouse was individually placed on a rotating rod, and the rotational speed was set to a low rate (5 rpm). The speed of the rod was gradually increased from 5 to 40 rpm over 5 min throughout the test. The latency to fall from the rotating rod was recorded and the average value of the two measurements was calculated.

2.5. Necrosis assay

Necrosis was assessed 1, 3, 7, 14, and 21 days post-surgery. On the day of measurement, the animals were anesthetized with isoflurane for respiratory anesthesia. Prior to blood perfusion measurement, the degree of ischemic symptoms in the ischemic hindlimb was visually scored using the following criteria[22] (Table 1):

Table 1. Necrosis severity scale

Score	Symptoms
0	No visible necrosis

1	Minor necrosis of the nail bed
2	Necrosis affecting all digits
3	Necrosis involving loss of at least one digit
4	Severe necrosis, loss of two or more digits, or significant foot necrosis

2.6. Perfusion ratio measurement

Blood perfusion measurements were conducted before surgery and 1, 3, 7, 14, and 21 days post-surgery. On the day of measurement, the animals were anesthetized with isoflurane, and a laser Doppler perfusion imaging system (LDPI) using a PeriScan PIM 3 (Perimed AB, Stockholm, Sweden) was used to measure blood perfusion in the hindlimbs. LDPI detects light scattered by the blood flow[23] and enables real-time monitoring of blood flow changes in the hindlimbs[24].

LDPI measurements were conducted on mice while maintaining their body temperature at 37 °C using a temperature control pad. At each time point, the LDPI probe was carefully positioned in the target region to ensure stable contact with the skin. The perfusion values were measured per pixel, and the captured images were processed using the LDPIwin software (Perimed AB) to calculate the blood perfusion ratio in the ischemic and non-ischemic limbs.

2.7. Inflammatory and angiogenic cytokine analyses

To assess the expression levels of cytokines related to inflammation regulation and angiogenesis, quantitative polymerase chain reaction (qPCR) was performed postoperatively on days 3, 7, 14, and 21. Inflammatory cytokines[25] (tumor necrosis factor-α (TNF-α), interleukin (IL)-1β, IL-6, and transforming growth factor (TGF)-β), and angiogenic cytokines (angiopoietins (ANG)-1, fibroblast growth factor (FGF), vascular endothelial growth factor (VEGF), and platelet-derived growth factor (PDGF)) were analyzed using qPCR[26].

Mice from each experimental group were euthanized and hindlimb tissues were carefully harvested. Total RNA was extracted from the hindlimb tissues using an RNA extraction kit (TRIzol LS Reagent, 15596026, Invitrogen, Carlsbad, CA, USA) as per the manufacturer's instructions. Reverse transcription was performed to synthesize complementary DNA (cDNA) from the extracted RNA using a cDNA synthesis kit (RevertAid First Strand cDNA Synthesis Kit, K1622, Thermo Fisher Scientific, Waltham, MA, USA). For real-time qPCR, the target gene transcript levels were quantified with SsoAdvanced Universal SYBR Green Supermix (1725275, Bio-Rad, Hercules, CA, USA) using the CFX384 Touch Real-Time PCR Detection System (Bio-Rad). Glyceraldehyde 3-phosphate dehydrogenase (GAPDH) was the internal control for normalization. The relative expression levels of target genes were calculated using the $\Delta\Delta C_T$ method[27]. The threshold cycle (C_T) is the fractional cycle number at which the amplified target reaches a fixed threshold. The primer sequences used for real-time PCR are listed in Table 2.

Table 2. Primer sequences for quantitative polymerase chain reaction

IL-1β	primer forward:	5′- GAT AAC CTG GTG TGT GA -3′
	primer reverse:	5′- GTT CAT CTC GGA GCC TGT AG -3′
IL-6	primer forward:	5′- TCA CAA GTC GGA GGC TTA ATT ACA -3′
	primer reverse:	5′- TGC ACA ACT CTT TTC TCA TTT CCA -3′
TNF-α	primer forward:	5′- CCC TGG CTG CCC TTC AC -3′
	primer reverse:	5′- TCA TTG AGG GCT TCT CTT GTT CT -3′
TGF-β1	primer forward:	5′- GAG CCC TGG ATA CCA ACT AT -3′
	primer reverse:	5′- AGA CAG AAG TTG GCA TGG TA -3′
ANG-1	primer forward:	5′- GGG GAG GTT GGA CAG TAA TA -3′
	primer reverse:	5′- AGC ATG TAC TGC CTC TGA CT -3′
FGF-2	primer forward:	5′- GCT GGC TTC TAA GTG TGT TA -3′
	primer reverse:	5′- AGT TTA TAC TGC CCA GTT CG -3′
VEGF	primer forward:	5′- GGT TTA AAT CCT GGA GCG TT -3′
	primer reverse:	5′- CGT TCG TTT AAC TCA AGC TG -3′
PDGF	primer forward:	5′- CAG ATC TCT CGG AAC CTC AT -3′
	primer reverse:	5′- CAC ATT GCG GTT ATT GCA G -3′
GAPDH	primer forward:	5′-TGA TGG GTG TGA ACC ACG AG -3′
	primer reverse:	5′-GAT GGC ATG GAC TGT GGT CA -3′
RNA extraction	TRIzol LS Reagent, Invitrogen	
cDNA synthesis	RevertAid first strand cDNA synthesis kit, Thermo Fisher Scientific	
PCR reagent	SsoAdvanced Universal SYBR Green Supermix	
qPCR conditions:	95 °C, 30 s	
	95 °C, 10 s	× 40 cycles
	60 °C, 20 s	
PCR instrument	CFX384 Touch Real-Time PCR Detection System, Bio-Rad Laboratories	

qPCR, quantitative polymerase chain reaction; Il, interleukin; TNF, tumor necrosis factor; TGF, tumor growth factor; ANG, angiopoietin; FGF, fibroblast growth factor; VEGF, vascularized endothelial growth factor; PDGF, platelet-derived growth factor; GAPDH, glyceraldehyde-3-phosphate.

2.8. Histological and immunohistochemistry (IHC) analyses

To evaluate muscle morphology and inflammation, hematoxylin and eosin (H&E) staining was performed using muscle tissue sections extracted on days 7, 14, and 21 following surgery[28,29]. The collected hindlimb tissues were fixed in 10% buffered formalin, embedded in paraffin blocks, and sectioned at 3–4 μm thickness. Masson's trichrome (MT) staining was performed to evaluate collagen deposition and fibrosis in muscle tissues. For assessing vascularization, IHC staining was performed using an anti-CD31 (endothelial cell marker for capillary density) and anti-α-smooth muscle actin (α-SMA, vascular smooth muscle cell marker for arteriole density).[30,31] Vessel density was expressed as the number of $CD31^+$ or SMA^+ cells per μm^2 of the analyzed muscle. Stained tissue sections were observed under a light microscope (Model Eclipse 80*i*, Nikon, Tokyo, Japan) equipped with a camera system (ProgRes C5, Jenoptik Optical Systems GmbH, Jena, Germany) and a computer-assisted automated image analyzer (*i*Solution FL ver 9.1, IMT *i*-solution Inc., BC, Canada).

2.9. Statistical analysis

Statistical analyses were performed using IBM SPSS software version 25.0 (IBM Corp., Armonk, NY, USA) and R software version 4.2.3 (R Foundation for Statistical Computing, Vienna, Austria). Data are presented as mean ± standard deviation. One-way analysis of variance (ANOVA) was performed to compare means of continuous variables among the five groups (G1–G5). If a one-way ANOVA showed a significant difference among the groups, post-hoc tests using Bonferroni correction were conducted to determine the specific groups that differed significantly from each other. Time effects were analyzed using repeated-measures ANOVA. A *p*-value of less than 0.05 was considered statistically significant.

3. RESULTS

3.1. E-MSC characterization

The E-MSC viability in G3, G4, and G5 were 89.9%, 93.0%, and 96.1%, respectively (Table 3).

Table 3. Live and total nucleated cell counts and viability in the E-MSC-treated groups.

Variables	Group 3[1]	Group 4[1]	Group 5[1]
Number of live cells (n)	6.35×10^4	1.39×10^5	2.11×10^5
Total cell count (n)	7.06×10^4	1.5×10^5	2.19×10^5
Viability[2] (%)	89.9%	93.0%	96.1%

[1]Groups 3, 4, and 5 represent cohorts administered E-MSC at low, medium, and high doses, respectively, following induction of ischemia. E-MSC yield was evaluated by counting total and live

nucleated E-MSCs using an automated cell counter.

[2]Cell viability (%) = (number of live cells / Total cell count) × 100; E-MSC, embryonic stem cell-derived mesenchymal stem cells.

Cell morphology after seeding for 6 days showed fibroblast-like cells attached to the plastic culture dish, indicating the mesenchymal nature of the E-MSCs (Figure 2A). Flow cytometry analysis using FITC- and PE-conjugated antibodies revealed the stromal characteristics of E-MSCs. Figure 2B shows a positive expression of CD29, CD44, CD73, and CD105, which are typical surface markers found on MSCs. These markers play crucial roles in various cellular processes such as adhesion, migration, survival, and immune modulation, suggesting the mesenchymal stem cell phenotype of E-MSCs and their potential for tissue repair and regeneration. Furthermore, the analysis revealed a lack of or reduced expression of hematopoietic markers CD34 and CD45, along with the absence of the antigen-presenting molecule human leukocyte antigen (HLA)-DR, commonly found on T cells and monocytes. Additionally, pluripotency-associated surface marker stage-specific embryonic antigen-3 (SSEA-3), tumor-related antigen (TRA)-1-60, and TRA-1-81 were either not detected or significantly diminished on E-MSCs, consistent with their embryonic stem cell origin. These results indicate the absence or downregulation of these markers on E-MSCs, reflecting their MSC-like characteristics rather than hematopoietic or pluripotent stem cell properties.

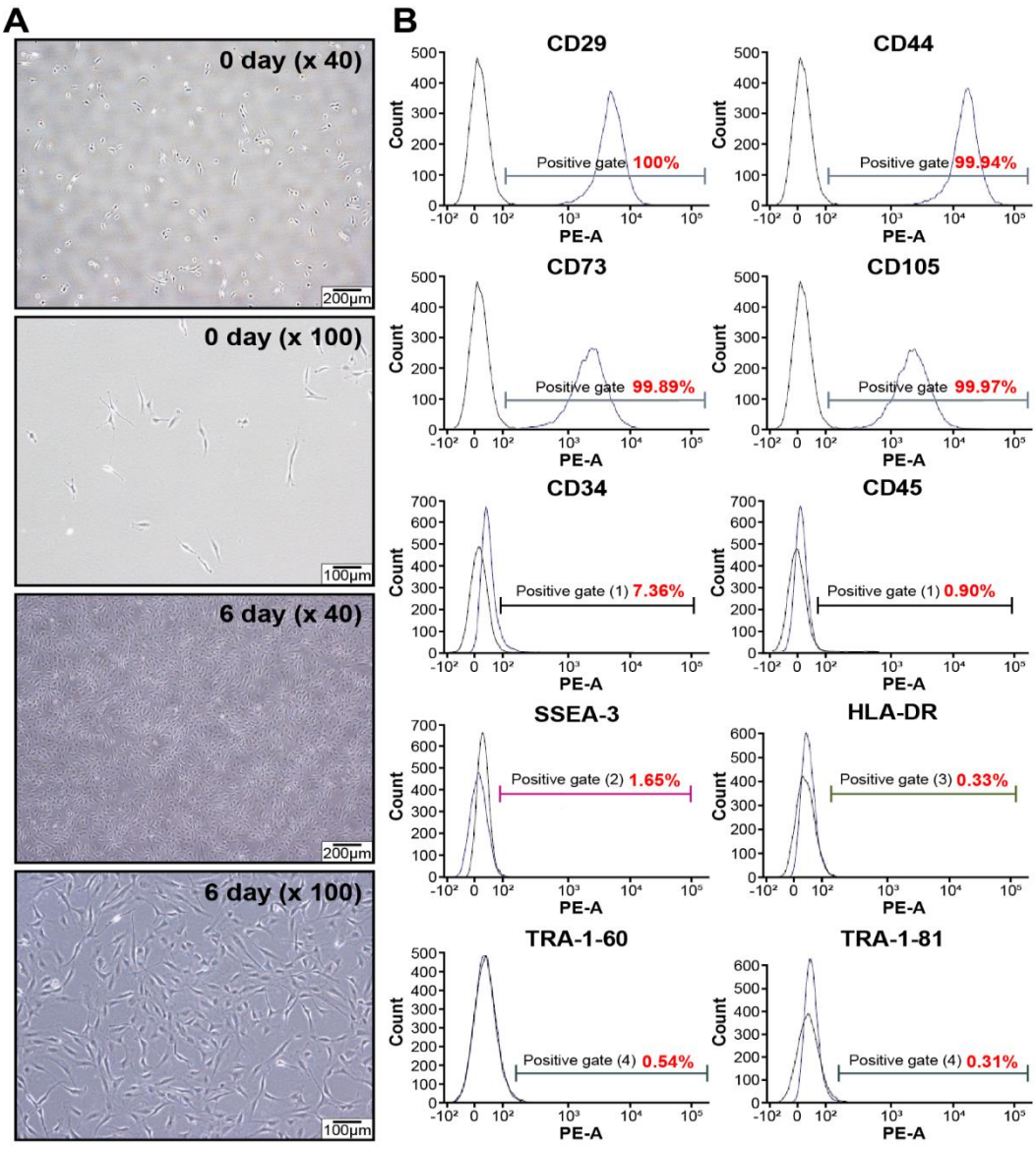

Figure 2. Characterization of embryonic stem cell-derived mesenchymal stem cells. (A) Morphology of E-MSCs after plating from day 1 to 6 (×40 and ×100 magnification, respectively). (B) Cell surface marker expression was measured using flow cytometry. The black lines indicate isotype-matched control staining. The blue lines represent cells stained with fluorescent dye-conjugated antibodies. E-MSCs strongly expressed CD29, CD44, CD73, and CD105 but negatively expressed CD34, CD45, SSEA-3, HLA-DR, TRA-1-60, and TRA-1-81.

HLA, human leukocyte antigen; PE-A, phycoerythrin-conjugated antibodies; SSEA, stage-specific embryonic antigen; TRA, tumor-related antigen.

3.2. Rotarod test

In the rotarod test (Figure 3), the non-ischemic group (sham group, G1) demonstrated normal motor coordination and balance at all time points, with no significant differences in the latency time. In contrast, the control group (G2) showed a sharp decrease in latency time on the first day after surgery, and it did not recover over time. Following surgery, the latency time in the E-MSC-treated groups (G3–G5) decreased, albeit to a lesser extent compared to G2 ($P < 0.05$). We observed that latency time gradually improved in the study groups after 7 days, although the difference was not statistically significant.

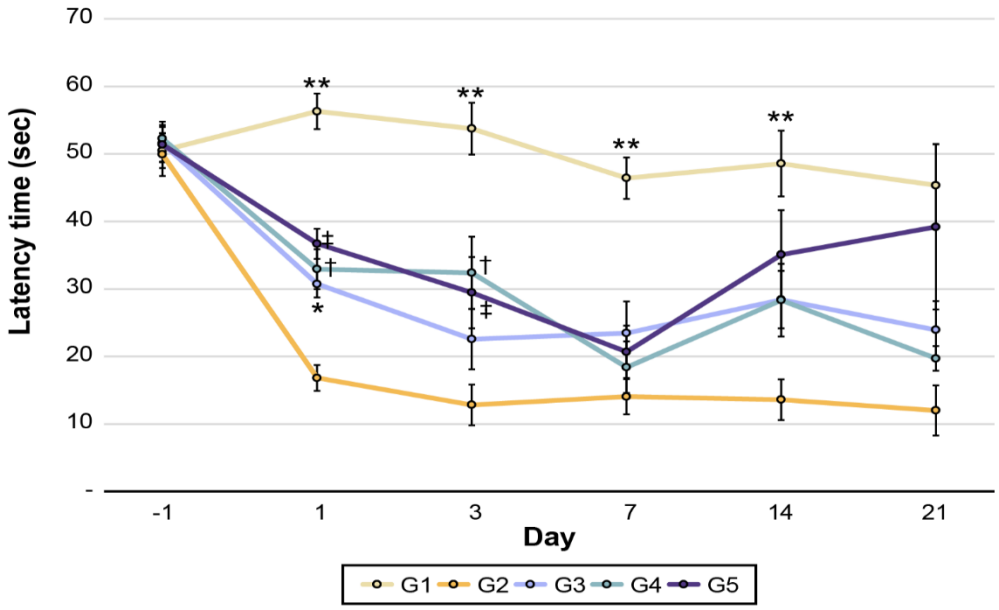

Figure 3. Changes in latency time in the rotarod test for each group. G1 serves as the sham group without inducing ischemia, whereas G2 acts as the control group with induced ischemia but treated with saline. The study groups, G3–5, induced ischemia and received low, medium, and high doses of E-MSCs, respectively. After ischemia induction, the latency time in the study groups (G3–G5) decreased to less than that in the control group (G2). No significant difference was observed in the latency time, according to E-MSC dose (** G1 vs. G2–G5, $P < 0.05$; * G2 vs. G3, $P < 0.05$; † G2 vs. G4, $P < 0.05$; ‡ G2 vs. G5, $P < 0.05$).

3.3. Necrosis assay

Necrosis assay showed that the non-ischemic group (G1) had no necrotic tissues. On the 7th day after ischemia induction, necrosis occurred in 42.9% (6/14) of the mice in G2; four mice experienced necrosis with a severity score of 2 or higher. Although no statistical significance was observed over time, one mouse in the surviving mice experienced a deterioration in necrosis score from 2 to 4 on day 14. Additionally, on day 21, 75% (3/4) of the surviving mice showed necrosis with a score of 1. In the E-MSC-treated groups, necrosis with a score of 2 or higher on day 7 was observed in 14.3%, 14.3%, and 21.4% of G3, G4, and G5, respectively. Over time, no new necrosis occurred in G3–G5; however, the scores for previously necrotic areas worsened (Figure 4).

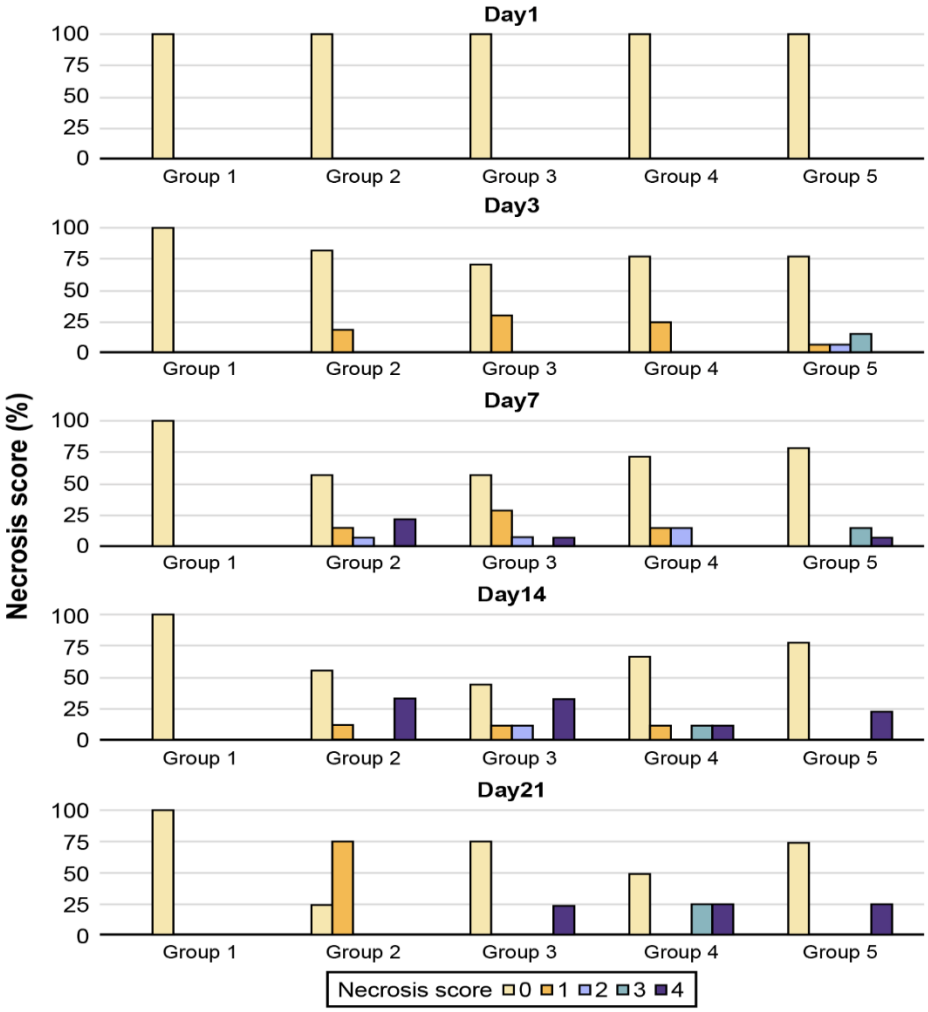

Figure 4. Changes in the necrosis score at each time point. Necrosis did not occur in the non-

ischemic group (G1), whereas in the ischemia-induced group (G2–G5), necrosis developed over time; however, no significant difference was observed among the ischemia-induced groups.
G2, saline-treated ischemia (control) group; G3, low-dose E-MSC-treated ischemia group; G4, medium-dose E-MSC-treated ischemia group, G5, high dose-E-MSC-treated ischemia group.

3.4. Blood perfusion ratio

The sham group (G1) showed almost the same level of blood perfusion compared with the normal limb; however, in the ischemia-induced groups (G2–G5), the perfusion ratio between normal and test limbs was significantly lower than that of G1 ($P < 0.05$). On days 7, 14, and 21, G2 showed a slight recovery in the perfusion ratio, although no statistical significance was observed. However, G3–G5 exhibited a significant improvement in the perfusion ratio over time compared with G2 ($P < 0.05$). The blood perfusion ratio showed the most significant recovery in the medium-dose E-MSC-treated group (G4), but no significant difference in the improvement of perfusion ratio was observed among G3, G4, and G5 (Figure 5).

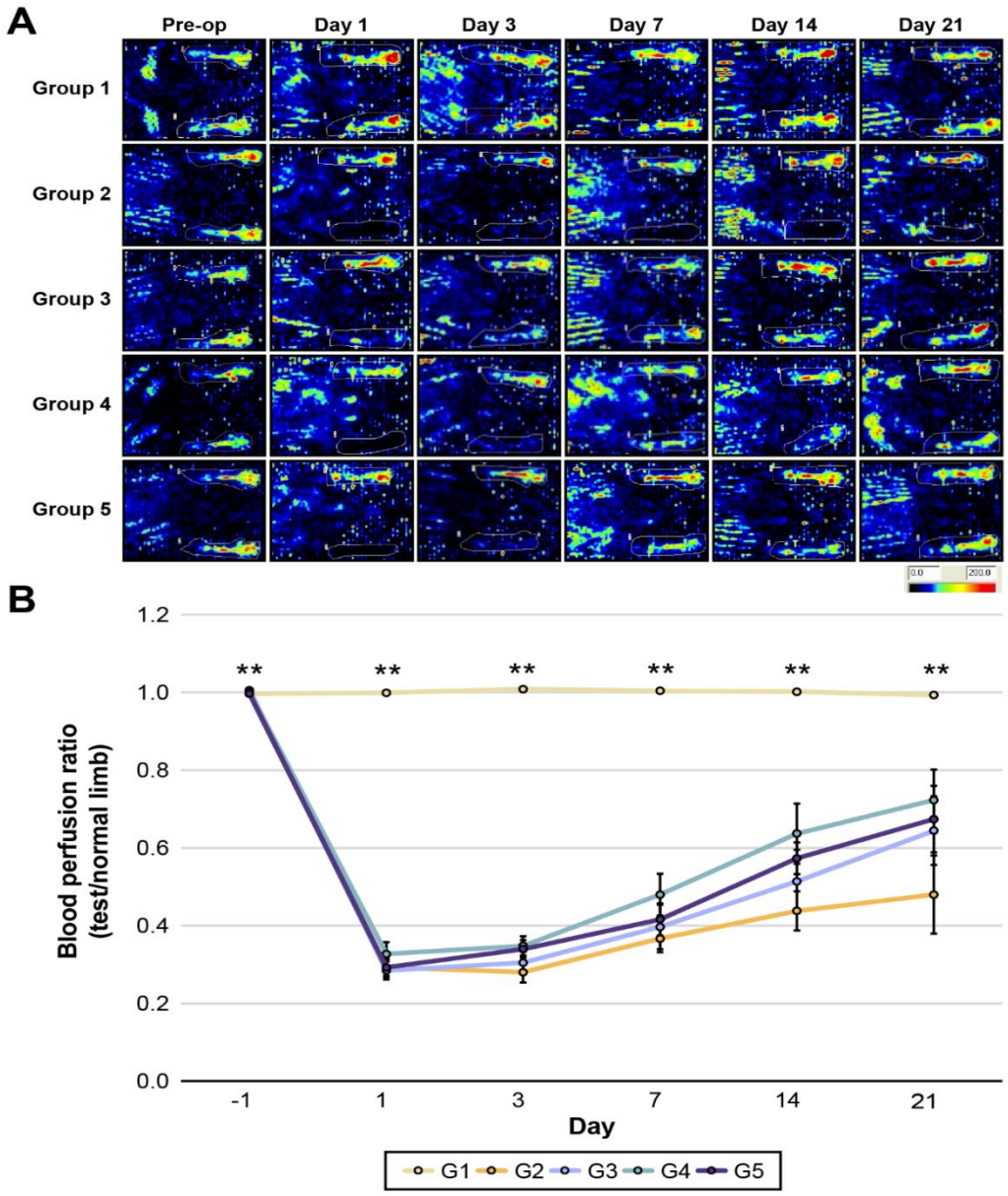

Figure 5. Assessment of the blood perfusion ratio. (A) Perfusion ratio in both hindlimbs obtained using laser doppler on days 1, 3, 7, 14, and 21 after cell injection. Dark blue indicates low to no blood perfusion, whereas red represents the highest perfusion level. (B) Changes in blood perfusion ratio over time. The perfusion ratio of the left limb (test) to the right limb (normal) improved gradually in the E-MSC-treated groups compared with that in the control group. However, no

significant difference was noted in perfusion ratio based on the dose of E-MSCs administered (** G1 vs. G2–G5, $P < 0.01$).
G1, non-ischemia (sham) group; G2, saline-treated ischemia (control) group; G3, low-dose E-MSC-treated ischemia group; G4, medium-dose E-MSC-treated ischemia group, G5, high dose-E-MSC-treated ischemia group.

3.5. Cytokine analysis

3.5.1. Inflammatory cytokines

In the qPCR analysis of inflammatory cytokines (Figure 6), the control group (G2) showed an increase in the mRNA expression levels of IL-1β, IL-6, TNF-α, and TGF-β compared to the sham group (G1), excluding day 7 for TGF-β. The study groups (G3–G5) exhibited a decrease in mRNA expression levels of inflammatory cytokines compared to the control group, although the difference was not statistically significant. On day 21, an increase in the mRNA expression of inflammatory cytokines was observed in the study and control groups.

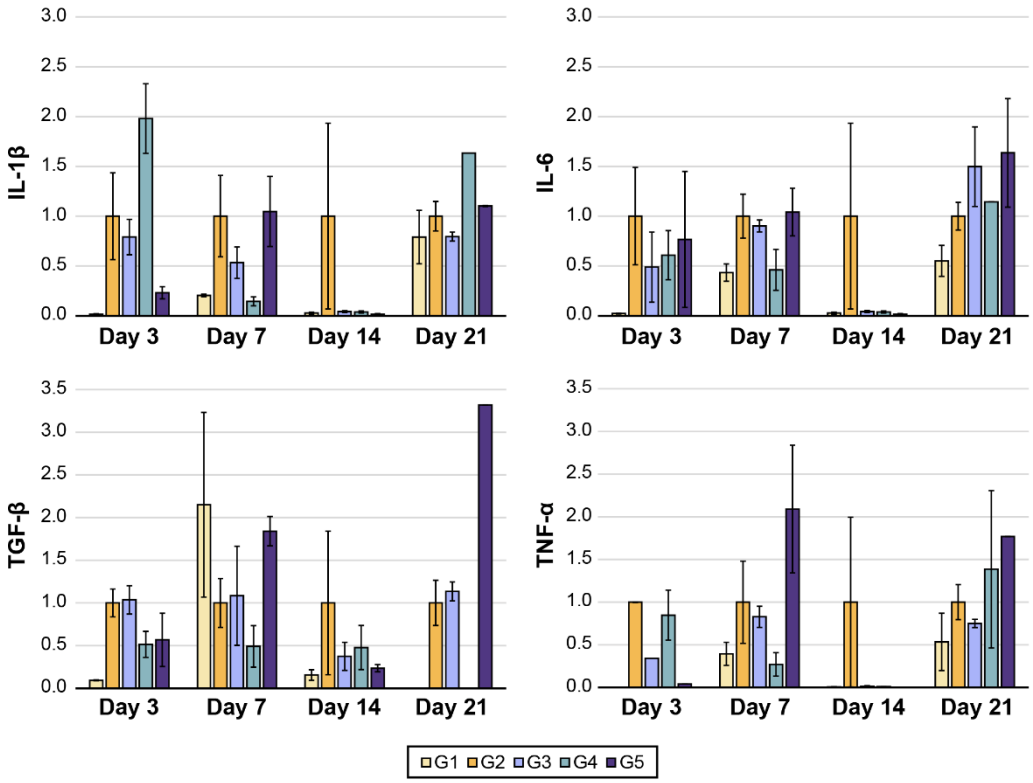

Figure 6. Inflammatory cytokine mRNA expression levels. The ischemia-induced groups (G2–G5) exhibited increased expression of inflammatory cytokines in the early stage.

While the mRNA expression in the study groups was lower compared to the control group, no significant differences were observed among the groups.
G1, non-ischemia (sham) group; G2, saline-treated ischemia (control) group; G3, low-dose E-MSC-treated ischemia group; G4, medium-dose E-MSC-treated ischemia group, G5, high dose-E-MSC-treated ischemia group.

3.5.2. Angiogenic cytokines

In the control group (G2), qPCR analysis showed elevated mRNA expression levels of angiogenic cytokines compared to those in the sham group (G1), excluding day 3 for VEGF. In the early stage, the E-MSC-treated groups (G3–G5) exhibited more increased mRNA expression levels of ANG1, FGF, VEGF, and PDGF compared with the control group (G2). Over time, the expression of angiogenic cytokines gradually decreased in the E-MSC-treated groups (G3–G5). The sham and study groups showed increased PDGF expression on days 14 and 21; however, the difference was not statistically significant (Figure 7).

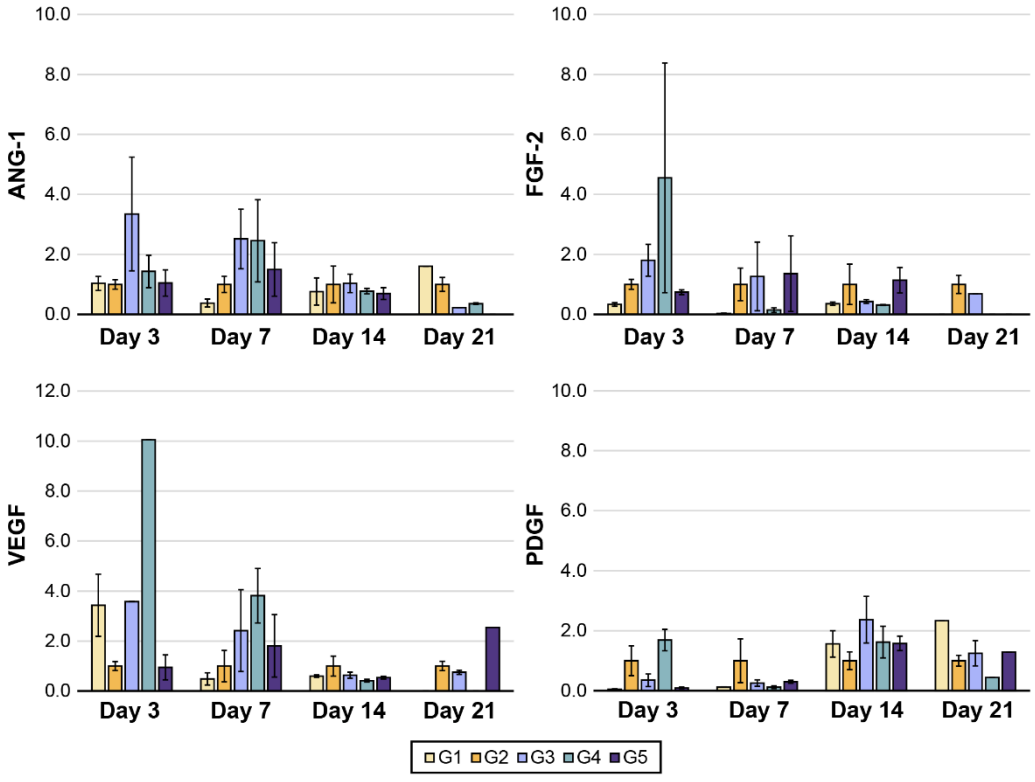

Figure 7. Angiogenic cytokine mRNA expression levels. The ischemia-induced groups (G2–G5) show an initial increase in the expression of angiogenic cytokines compared to the sham group.

However, no significant difference was observed based on the dose of E-MSCs.
G1, non-ischemia (sham) group; G2, saline-treated ischemia (control) group; G3, low-dose E-MSC-treated ischemia group; G4, medium-dose E-MSC-treated ischemia group, G5, high dose-E-MSC-treated ischemia group.

3.6. Histological analysis

We analyzed myofiber thickness, number, and infiltrated inflammatory cell count using H&E staining; the results are presented in Table 4.

Table 4. Myofiber thickness, myofiber number, and infiltrated inflammatory cell count resulting from the hematoxylin and eosin (H&E) analysis.

	G1	G2	G3	G4	G5	*P*-value[1]
Myofiber thickness (μm)						
Day 7	39.3±0.4	26.6±2.7	26.0±0.1	24.8±3.4	24.7±1.5	0.004*
Day 14	34.8±2.0	30.0±0.4	26.8±0.4	29.2±5.3	33.8±5.8	0.294
Day 21	38.8±1.9	29.1±6.0	27.1±3.6	27.7±2.1	31.2±2.8	0.101
Myofiber number (myofiber/mm^2)						
Day 7	335.0±12.7	159.0±63.6	98.0±19.8	198.0±62.2	150.0±53.7	0.027†
Day 14	339.0±1.4	186.0±42.4	195.0±63.6	120.0±79.1	207.5±53.0	0.071
Day 21	334.0±2.8	137.0±72.1	319.0±12.7	232.0±33.9	184.0±22.6	0.011‡
Infiltrated inflammatory cell number (cells/mm^2)						
Day 7	7.0±1.4	319±182.4	362±124.5	195±173.9	283±21.2	0.172
Day 14	8.0±2.8	64.0±28.3	176±186.7	181±179.6	46.0±17.0	0.522
Day 21	8.0±0.1	170±155.6	46±8.5	47.0±15.6	40.0±16.9	0.314

[1]Where any significant change was identified using analysis of variance (ANOVA), post-hoc analysis using Bonferroni multiple comparisons was used to confirm any significant group differences.
* All adjusted *P*-values for comparisons of G1 vs. G2, G1 vs. G3, G1 vs. G4, and G1 vs. G5 are < 0.05.
† G1 vs G3, adjusted $P = 0.042$.
‡ G1 vs G2, adjusted $P = 0.027$, G2 vs G3, adjusted $P = 0.047$.
G1, non-ischemia (sham) group; G2, saline-treated ischemia (control) group; G3, low-dose E-MSC-treated ischemia group; G4, medium-dose E-MSC-treated ischemia group, G5, high dose-E-MSC-treated ischemia group.

On postoperative day 7, myofiber thickness decreased significantly in the ischemia-induced

groups (G2–G5) compared to the sham group (G1), with no significant difference observed between E-MSC-treated (G3–G5) and control (G2) groups. However, on postoperative days 14 and 21, no significant differences were observed in myofiber thickness between the ischemia-induced (G2–G5) and sham (G1) groups.

The myofiber number decreased, particularly in the low-dose E-MSC-treated group (G3) on day 7, although no significant difference was observed between G2 and G3–G5. By day 21, the myofiber number in G3 was significantly higher than that in G2 ($P = 0.011$). Overall, no significant differences were observed in myofiber number among the groups treated with different doses of E-MSCs throughout the study period. On postoperative day 7, the ischemia-induced groups (G2–G5) showed increased infiltrated inflammatory cell counts and the area of MT-stained collagen fibers compared to that in G1. However, by day 21, the number of infiltrated inflammatory cells and the area of MT-stained collagen fibers significantly decreased in E-MSC-treated groups (G3–G5) compared to that in G2 (Figure 8).

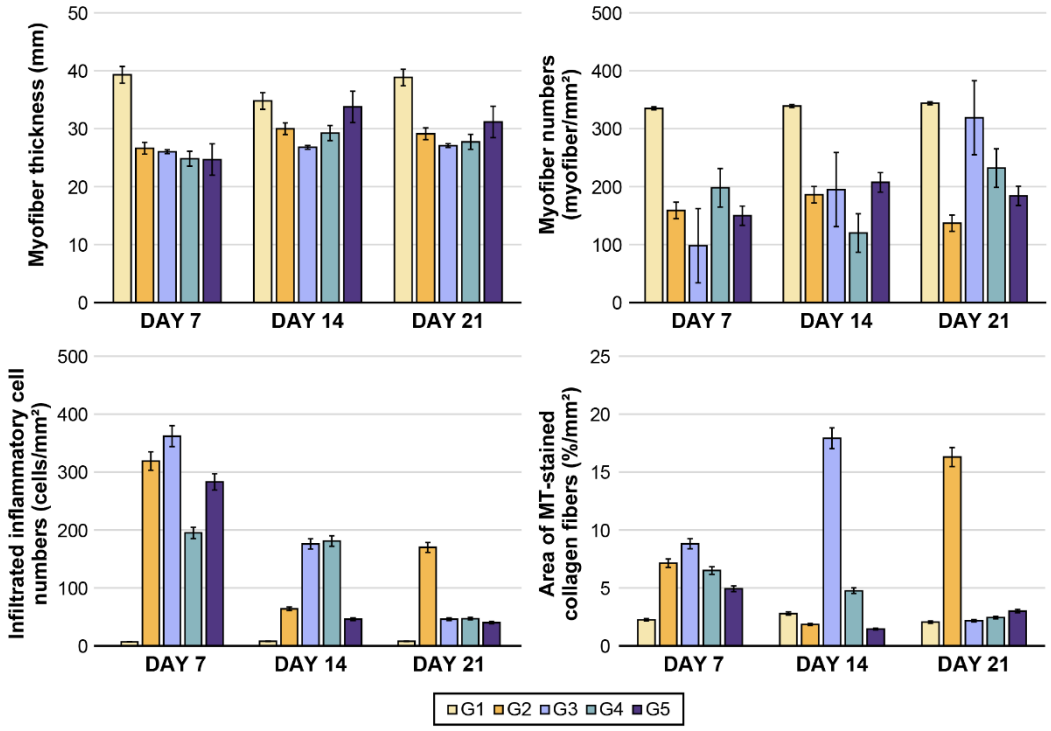

Figure 8. Histological analysis in muscle tissues. Compared to the sham group, the ischemia-induced groups (G2–G5) showed a decrease in myofiber thickness and myofiber number, along with an increase in infiltrated inflammatory cell counts. On days 7 and 21, the area of Masson's trichrome (MT)-stained collagen fibers increased in G2 compared to G1. However, the study group (G3–G5) showed a decrease in the area of MT-stained collagen fibers compared to G2. In addition, no

significant differences were observed across all variables based on the dose of E-MSCs.
G1, non-ischemia (sham) group; G2, saline-treated ischemia (control) group; G3, low-dose E-MSC-treated ischemia group; G4, medium-dose E-MSC-treated ischemia group, G5, high dose-E-MSC-treated ischemia group.

The images of the overall histological analysis are presented in Figure 9.

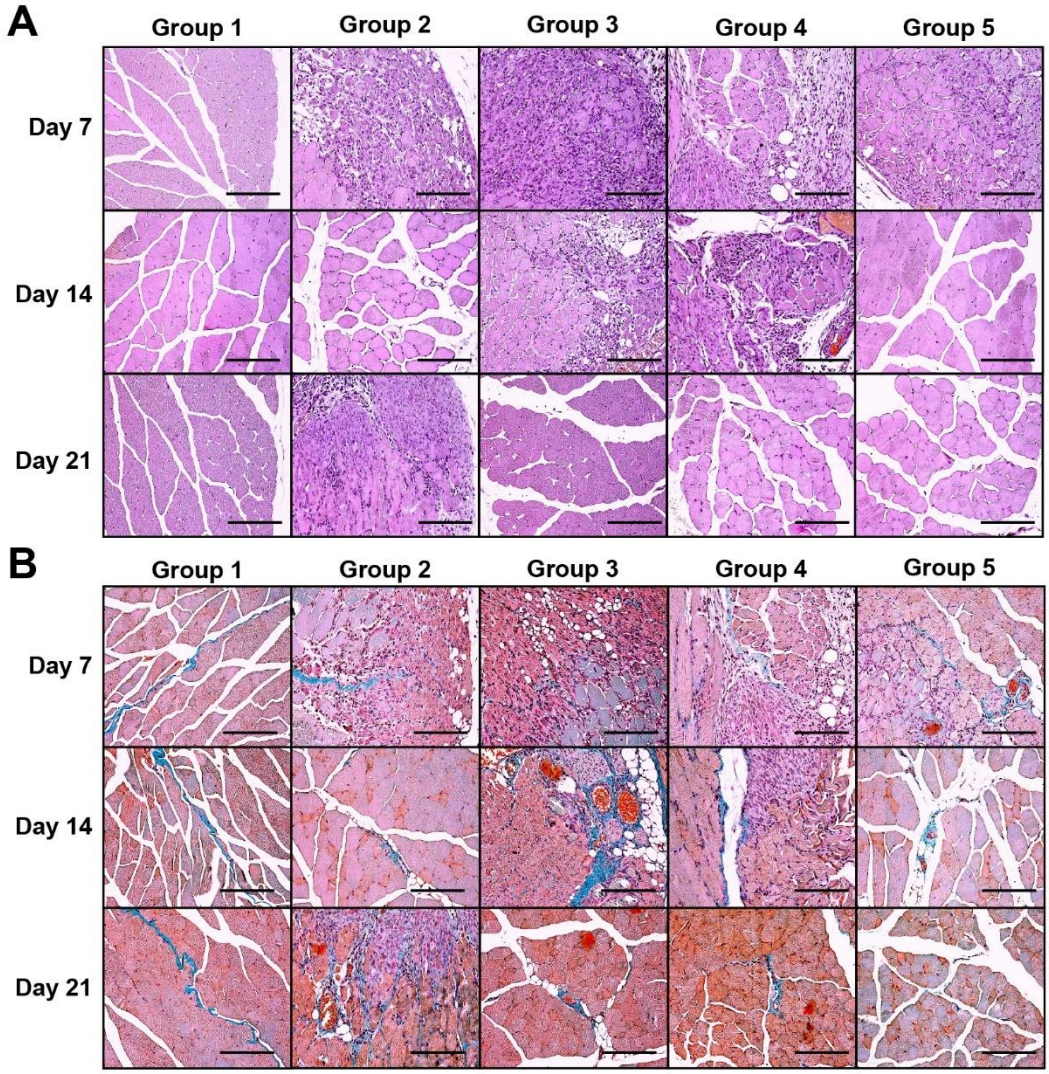

Figure 9. Immunohistochemistry staining images for each group. (A) Hematoxylin and eosin (H&E) and (B) Masson's trichrome (MT) staining for ischemic muscle (×200 magnification). In H&E staining, infiltrated inflammatory cells appear as dark purple within the tissue, whereas in MT

staining, collagen fibers are depicted in blue.
Group 1, non-ischemia (sham) group; Group 2, saline-treated ischemia (control) group; Group 3, low-dose E-MSC-treated ischemia group; Group 4, medium-dose E-MSC-treated ischemia group, Group 5, high dose-E-MSC-treated ischemia group.

3.7. IHC analysis

G2 exhibited a decreased density of CD31+ capillaries compared to G1, whereas no significant changes were observed in the α-SMA+ arteriole density between the control (G2) and sham groups (G1) (Figure 10).

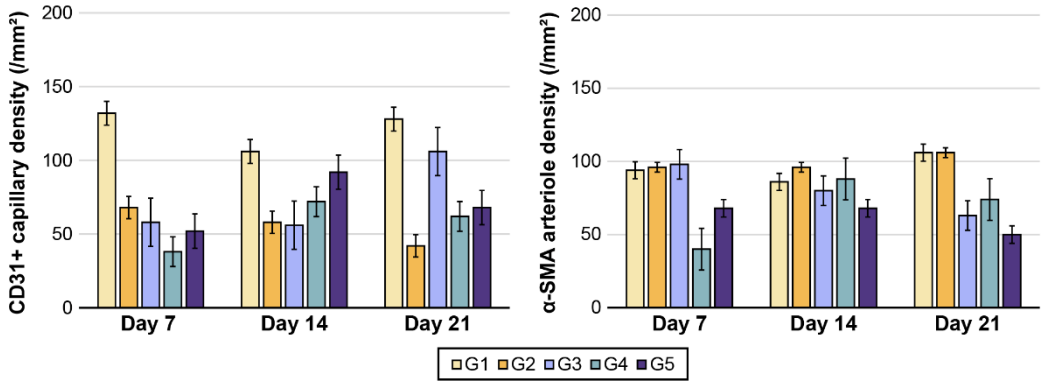

Figure 10. Capillary and arteriole density in muscle tissue. On day 7, the ischemia-induced groups (G2–G5) exhibited a decreased CD31+ capillary density compared to G1, but no difference in capillary density was observed among the G2–G5 groups. The α-smooth muscle actin (α-SMA) arteriole density was similar across all groups.
G1, non-ischemia (sham) group; G2, saline-treated ischemia (control) group; G3, low-dose E-MSC-treated ischemia group; G4, medium-dose E-MSC-treated ischemia group, G5, high dose-E-MSC-treated ischemia group.

However, on day 21, the E-MSC-treated groups (G3–G5) showed increased CD31+ capillary density and decreased α-SMA+ arteriole density compared to G2 (Figure 11).

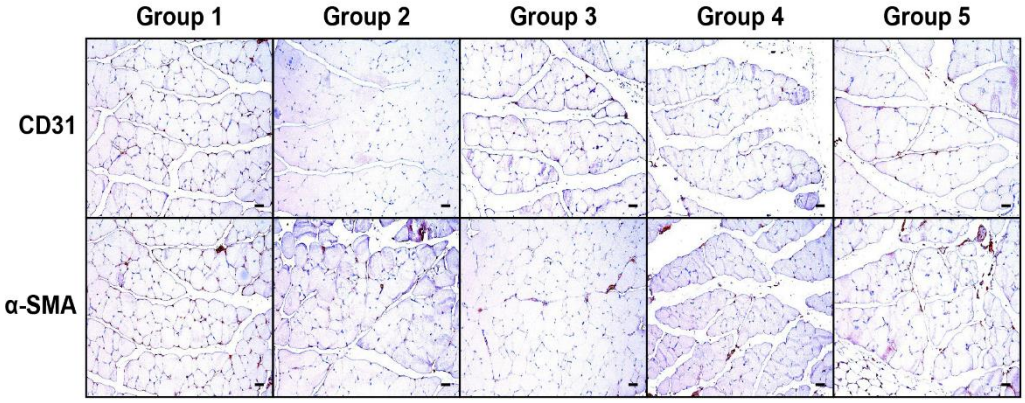

Figure 11. CD31 and α-SMA staining images on day 21. The capillary and arteriole appear brown in color in the image (×200 magnification).
Group 1, non-ischemia (sham) group; Group 2, saline-treated ischemia (control) group; Group 3, low-dose E-MSC-treated ischemia group; Group 4, medium-dose E-MSC-treated ischemia group, Group 5, high dose-E-MSC-treated ischemia group.

4. DISCUSSION

This study evaluated the therapeutic effects of E-MSCs in a murine hindlimb ischemia model and investigated the potential differences based on E-MSC dose. Key findings revealed that E-MSC transplantation improved blood perfusion, enhanced motor function, and increased microvessel density in ischemic limbs. Additionally, the E-MSC-treated ischemia group showed substantial reductions in inflammatory cytokines (TNF-α, IL-1β, IL-6, and TGF-β) and notable increases in angiogenetic cytokines (ANG1, FGF, VEGF, and PDGF) compared to the control group. However, discernible differences in therapeutic effects based on E-MSC dosage were not observed.

Stem cell-based therapies are a promising avenue for patients who are unsuitable for surgery or those with limited options for endovascular procedures[2]. With their regenerative and paracrine effects, MSCs may address the intricate pathophysiology of CLTI and other cardiovascular diseases[7,8]. Paracrine effects, mediated by the secretion of growth factors, cytokines, and extracellular vesicles, are pivotal in promoting angiogenesis, modulating inflammation, and enhancing tissue repair[32,33]. MSCs are derived from various sources, such as the umbilical cord, placenta, adipose tissue, bone marrow, and induced pluripotent stem cells[34,35]. This study focused on the angiogenesis and anti-inflammatory effects of E-MSCs mediated by paracrine activity.

Several studies have shown that MSCs can alleviate tissue damage and promote functional recovery following ischemic injury[14,36,37]. In line with these previous results, injecting E-MSCs into the ischemic limb recovered blood perfusion over time and improved the latency time of ischemic limbs in the current study. The capacity to improve blood flow is crucial for promoting tissue healing and reducing hindlimb ischemia severity. In that context, the E-MSC-treated group showed

improved functional outcomes, with higher capillary and arteriole densities in ischemic muscle post-treatment. This suggests that E-MSCs can mitigate tissue damage by promoting tissue repair and neovascularization[13]. However, in the necrosis assay, the control group had a lower average score on day 21 post-surgery compared to the E-MSC-treated group. This could be owing to higher-scoring mice being included in the mid-sacrifice group of G2, leaving relatively lower-scoring mice for days 14 and 21. In our study, E-MSC administration at a dose of 5.0×10^6 cells/kg showed the most significant improvement in blood perfusion, although no significant differences were observed in other concomitantly assessed variables compared to other concentrations. To effectively apply MSCs in clinical trials for CLTI[8,38], further research is needed on the cell dose, cell type, and administration time.

Ischemia induces tissue damage and triggers the inflammatory response as a natural defense mechanism[39]. We observed increased expression of pro-inflammatory cytokines (TNF-α, IL-1β, and IL-6) in the ischemic condition, indicative of acute inflammatory activation. This inflammatory cascade may exacerbate ischemic conditions, causing severe tissue damage. However, in the E-MSC-treated groups, the expression of TNF-α, IL-1β, and IL-6 reduced, suggesting the immunomodulatory potential of E-MSC therapy in dampening the inflammatory response. Furthermore, MSCs possess immunomodulatory properties by secreting factors like TGF-β, which inhibits lymphocyte activation and aids in suppressing inflammation[40]. The observed higher expression of TGF-β in the sham group on day 7 could be attributed to external factors such as physical activity or physiological conditions contributing to an increase in the tissue inflammatory response. The sustained expression of TGF-β in the control group suggests ongoing inflammation owing to persistent ischemia or delayed TGF-β degradation or metabolism. By day 21, the study and control groups showed increased expression of inflammatory cytokines, possibly indicating inflammation resurgence during tissue remodeling and recovery. TGF-β, known for its pleiotropic effects, may exhibit increased expression in the context of tissue injury[41,42]. This cytokine plays a pivotal role in regulating crucial processes, including cell growth, differentiation, immune modulation, inflammation suppression, extracellular matrix remodeling, tissue repair, and regeneration[43,44]. Hence, using E-MSCs in ischemic limbs may promote tissue healing and restoration of damaged structures via the secretion of paracrine factors such as TGF-β.

Previous studies have indicated that MSCs promote angiogenesis largely through pro-angiogenic factor secretion[45-47]. After the initial MSC administration, levels of angiogenic factors such as ANG1, FGF, VEGF, and PDGF increase, owing to the inflammatory response triggered by tissue damage or ischemia[46,47]. This initial surge is a natural reaction to promote neovascularization and tissue repair[48]. These factors promote angiogenesis, from recruiting endothelial cells to maturing blood vessels. In our findings, the increased expression of angiogenic factors in the early stages in the E-MSC-treated groups, compared to the control group, shows the therapeutic angiogenic potential of E-MSCs. However, these effects were not sustained beyond day 21. This suggests a potential decline in angiogenic efficacy over time, possibly because of adaptation and feedback mechanisms within the ischemic tissue. Moreover, for enduring vascular regeneration and tissue recovery in ischemic conditions, repeated administrations of E-MSCs might be necessary, hinting at the potential requirement for multiple doses.

Additionally, the higher expression of VEGF in the sham group compared to the control group on day 3 may result from a transient surge induced by tissue damage during surgery and physiological stress in the mice. VEGF is crucial for angiogenesis by promoting neovessel maturation and regulates endothelial cell-matrix interactions[47]. FGF contributes to angiogenesis and wound healing[49]. PDGF induces migration and proliferation of mural progenitor cells, stimulates endothelial cells, and triggers mesenchymal cell transformation into vessel cells[50]. These changes in angiogenic markers reflect the dynamic interaction between MSCs and the host tissue microenvironment[51], highlighting the ability of MSCs to finely regulate neovascularization and promote a balanced vascular response[52].

Ischemia induces tissue damage and initiates cellular responses, including the recruitment and activation of SMA, to aid the repair process[53]. This increases the expression of α-SMA, a marker of vascular SMA[34], suggesting that MSCs may actively contribute to arteriole formation. Arterioles promote neovascularization and restore blood flow in ischemic tissues, which may explain the marked improvement in blood perfusion observed in the E-MSC-treated groups. However, this study indicated a slight decrease in α-SMA expression, suggesting that rather than the formation of new vessels, blood flow may have improved because of the development of existing vasculature. Furthermore, positive expression of the endothelial cell marker CD31 suggests the potential differentiation of E-MSCs into endothelial-like cells in the ischemic limb. These findings demonstrate that E-MSCs may contribute to the essential process of angiogenesis, which is vital for tissue repair and regeneration.

This study had some limitations. First, immune rejection-related concerns are present, as embryonic stem cell-derived therapies may trigger an immune response in the recipient[54,55]. Although we did not observe any signs of immune rejection or tissue inflammation during the experimental period, future studies should explore immunomodulatory strategies to enhance the engraftment and survival of transplanted E-MSCs. Second, monitoring the tumorigenic potential of embryonic stem cells is crucial[40,56], and hence requires rigorous safety assessments and long-term follow-up to prevent adverse effects, including tumor formation. Third, this study encountered discrepancies between functional outcomes, such as motor coordination improvement and blood perfusion recovery, as well as anatomical outcomes observed through molecular analysis. Biases during the hindlimb ischemia model creation might have contributed to these inconsistencies. Isoflurane, known to induce ischemic preconditioning, typically safeguards tissues such as the brain, retina, heart, and lungs by temporarily reducing blood flow and mitigating oxidative stress and inflammation. Thus, its effects could alter tissue responses and serve as a confounding factor, potentially distorting the observed effects of E-MSCs. Moreover, murine models may not fully reflect the complexity of human physiology. The differences in lifespan between mice (approximately 2–3 years) and humans (approximately 80 years), anatomical variations in vascular structure and hemodynamics, as well as variations in the degree of ischemia, could also impact study outcomes. We standardized the experimental environment and conditions and ensured that tissue handling and surgical procedures were performed by a single experimenter to minimize bias. Finally, E-MSCs in tissue were not labeled; thus, their potential for differentiation into vascular-forming cells could not be identified using molecular imaging or immunohistochemistry. Additional

experiments involving repeated administration of E-MSCs at various dosages and confirmation of E-MSC viability inside the mice using fluorescent labeling may be warranted to clearly ascertain the therapeutic effect (paracrine effect) of E-MSCs.

5. CONCLUSION

Our study established an ischemic hindlimb murine model using BALB/c nude mice and evaluated the therapeutic potential of MSC therapy at various concentrations. E-MSCs are promising candidates for promoting tissue repair, angiogenesis, blood perfusion, and functional recovery under ischemic conditions, offering a potential new treatment option for patients facing limited therapeutic choices in CLTI. However, given that the favorable effects of E-MSCs do not endure over time, additional large-scale studies are needed to explore the therapeutic efficacy of repeated dosing and ensure the safety of E-MSCs for clinical application.

REFERENCES

1 Norgren L, Hiatt WR, Dormandy JA, Nehler MR, Harris KA, Fowkes FG, et al. Inter-Society Consensus for the Management of Peripheral Arterial Disease (TASC II). *J Vasc Surg* 2007;**45 Suppl S**:S5-67.

2 Conte MS, Bradbury AW, Kolh P, White JV, Dick F, Fitridge R, et al. Global vascular guidelines on the management of chronic limb-threatening ischemia. *J Vasc Surg* 2019;**69**:3S-125S e40.

3 Howard DP, Banerjee A, Fairhead JF, Hands L, Silver LE, Rothwell PM, et al. Population-Based Study of Incidence, Risk Factors, Outcome, and Prognosis of Ischemic Peripheral Arterial Events: Implications for Prevention. *Circulation* 2015;**132**:1805-15.

4 Baubeta Fridh E, Andersson M, Thuresson M, Sigvant B, Kragsterman B, Johansson S, et al. Editor's Choice - Impact of Comorbidity, Medication, and Gender on Amputation Rate Following Revascularisation for Chronic Limb Threatening Ischaemia. *Eur J Vasc Endovasc Surg* 2018;**56**:681-8.

5 Vartanian SM, Conte MS. Surgical intervention for peripheral arterial disease. *Circ Res* 2015;**116**:1614-28.

6 Conte MS. Bypass versus Angioplasty in Severe Ischaemia of the Leg (BASIL) and the (hoped for) dawn of evidence-based treatment for advanced limb ischemia. *J Vasc Surg* 2010;**51**:69S-75S.

7 Giordano A, Galderisi U, Marino IR. From the laboratory bench to the patient's bedside: an update on clinical trials with mesenchymal stem cells. *J Cell Physiol* 2007;**211**:27-35.

8 Elshaer SL, Bahram SH, Rajashekar P, Gangaraju R, El-Remessy AB. Modulation of Mesenchymal Stem Cells for Enhanced Therapeutic Utility in Ischemic Vascular Diseases. *Int J Mol Sci* 2021;**23**.

9 Madrigal M, Rao KS, Riordan NH. A review of therapeutic effects of mesenchymal stem cell secretions and induction of secretory modification by different culture methods. *J Transl Med* 2014;**12**:260.

10 Zhao L, Johnson T, Liu D. Therapeutic angiogenesis of adipose-derived stem cells for ischemic diseases. *Stem Cell Res Ther* 2017;**8**:125.

11 Hawkins KE, Corcelli M, Dowding K, Ranzoni AM, Vlahova F, Hau KL, et al. Embryonic Stem Cell-Derived Mesenchymal Stem Cells (MSCs) Have a Superior Neuroprotective Capacity Over Fetal MSCs in the Hypoxic-Ischemic Mouse Brain. *Stem Cells Transl Med* 2018;**7**:439-49.

12 Trivedi P, Hematti P. Derivation and immunological characterization of mesenchymal stromal cells from human embryonic stem cells. *Exp Hematol* 2008;**36**:350-9.

13 Shirbaghaee Z, Hassani M, Heidari Keshel S, Soleimani M. Emerging roles of mesenchymal stem cell therapy in patients with critical limb ischemia. *Stem Cell Res Ther* 2022;**13**:462.

14 Laurila JP, Laatikainen L, Castellone MD, Trivedi P, Heikkila J, Hinkkanen A, et al. Human embryonic stem cell-derived mesenchymal stromal cell transplantation in a rat hind limb

injury model. *Cytotherapy* 2009;**11**:726-37.

15 Hong KS, Bae D, Choi Y, Kang SW, Moon SH, Lee HT, et al. A porous membrane-mediated isolation of mesenchymal stem cells from human embryonic stem cells. *Tissue Eng Part C Methods* 2015;**21**:322-9.

16 Kim DJ, Hahn HM, Youn YN, Lee JS, Lee IJ, Lim SH. Adipose Derived Stromal Vascular Fraction and Mesenchymal Stem Cells Improve Angiogenesis in a Rat Hindlimb Ischaemia Model. *Eur J Vasc Endovasc Surg* 2024;**67**:828-37.

17 Liew A, O'Brien T. Therapeutic potential for mesenchymal stem cell transplantation in critical limb ischemia. *Stem Cell Res Ther* 2012;**3**:28.

18 Lee EJ, Lee HN, Kang HJ, Kim KH, Hur J, Cho HJ, et al. Novel embryoid body-based method to derive mesenchymal stem cells from human embryonic stem cells. *Tissue Eng Part A* 2010;**16**:705-15.

19 Dominici M, Le Blanc K, Mueller I, Slaper-Cortenbach I, Marini F, Krause D, et al. Minimal criteria for defining multipotent mesenchymal stromal cells. The International Society for Cellular Therapy position statement. *Cytotherapy* 2006;**8**:315-7.

20 Kochi T, Imai Y, Takeda A, Watanabe Y, Mori S, Tachi M, et al. Characterization of the arterial anatomy of the murine hindlimb: functional role in the design and understanding of ischemia models. *PLoS One* 2013;**8**:e84047.

21 Deacon RM. Measuring motor coordination in mice. *J Vis Exp* 2013:e2609.

22 Bir SC, Pattillo CB, Pardue S, Kolluru GK, Shen X, Giordano T, et al. Nitrite anion therapy protects against chronic ischemic tissue injury in db/db diabetic mice in a NO/VEGF-dependent manner. *Diabetes* 2014;**63**:270-81.

23 Eriksson S, Nilsson J, Sturesson C. Non-invasive imaging of microcirculation: a technology review. *Med Devices (Auckl)* 2014;**7**:445-52.

24 Aref Z, de Vries MR, Quax PHA. Variations in Surgical Procedures for Inducing Hind Limb Ischemia in Mice and the Impact of These Variations on Neovascularization Assessment. *Int J Mol Sci* 2019;**20**.

25 Ucuzian AA, Gassman AA, East AT, Greisler HP. Molecular mediators of angiogenesis. *J Burn Care Res* 2010;**31**:158-75.

26 Pereira AR, Mendes TF, Ministro A, Teixeira M, Filipe M, Santos JM, et al. Therapeutic angiogenesis induced by human umbilical cord tissue-derived mesenchymal stromal cells in a murine model of hindlimb ischemia. *Stem Cell Res Ther* 2016;**7**:145.

27 Livak KJ, Schmittgen TD. Analysis of relative gene expression data using real-time quantitative PCR and the 2(-Delta Delta C(T)) Method. *Methods* 2001;**25**:402-8.

28 Makarevich P, Tsokolaeva Z, Shevelev A, Rybalkin I, Shevchenko E, Beloglazova I, et al. Combined transfer of human VEGF165 and HGF genes renders potent angiogenic effect in ischemic skeletal muscle. *PLoS One* 2012;**7**:e38776.

29 McClung JM, McCord TJ, Southerland K, Schmidt CA, Padgett ME, Ryan TE, et al. Subacute limb ischemia induces skeletal muscle injury in genetically susceptible mice independent of vascular density. *J Vasc Surg* 2016;**64**:1101-11 e2.

30 Huang WH, Chen HL, Huang PH, Yew TL, Lin MW, Lin SJ, et al. Hypoxic mesenchymal

stem cells engraft and ameliorate limb ischaemia in allogeneic recipients. *Cardiovasc Res* 2014;**101**:266-76.

31 Nossent AY, Bastiaansen AJ, Peters EA, de Vries MR, Aref Z, Welten SM, et al. CCR7-CCL19/CCL21 Axis is Essential for Effective Arteriogenesis in a Murine Model of Hindlimb Ischemia. *J Am Heart Assoc* 2017;**6**.

32 Chang C, Yan J, Yao Z, Zhang C, Li X, Mao HQ. Effects of Mesenchymal Stem Cell-Derived Paracrine Signals and Their Delivery Strategies. *Adv Healthc Mater* 2021;**10**:e2001689.

33 Mabotuwana NS, Rech L, Lim J, Hardy SA, Murtha LA, Rainer PP, et al. Paracrine Factors Released by Stem Cells of Mesenchymal Origin and their Effects in Cardiovascular Disease: A Systematic Review of Pre-clinical Studies. *Stem Cell Rev Rep* 2022;**18**:2606-28.

34 Lian Q, Zhang Y, Zhang J, Zhang HK, Wu X, Zhang Y, et al. Functional mesenchymal stem cells derived from human induced pluripotent stem cells attenuate limb ischemia in mice. *Circulation* 2010;**121**:1113-23.

35 Hu GW, Li Q, Niu X, Hu B, Liu J, Zhou SM, et al. Exosomes secreted by human-induced pluripotent stem cell-derived mesenchymal stem cells attenuate limb ischemia by promoting angiogenesis in mice. *Stem Cell Res Ther* 2015;**6**:10.

36 Gruenloh W, Kambal A, Sondergaard C, McGee J, Nacey C, Kalomoiris S, et al. Characterization and in vivo testing of mesenchymal stem cells derived from human embryonic stem cells. *Tissue Eng Part A* 2011;**17**:1517-25.

37 Yamahara K, Harada K, Ohshima M, Ishikane S, Ohnishi S, Tsuda H, et al. Comparison of angiogenic, cytoprotective, and immunosuppressive properties of human amnion- and chorion-derived mesenchymal stem cells. *PLoS One* 2014;**9**:e88319.

38 Han KH, Kim AK, Kim DI. Therapeutic Potential of Human Mesenchymal Stem Cells for Treating Ischemic Limb Diseases. *Int J Stem Cells* 2016;**9**:163-8.

39 Dimitrova E, Caromile LA, Laubenbacher R, Shapiro LH. The innate immune response to ischemic injury: a multiscale modeling perspective. *BMC Syst Biol* 2018;**12**:50.

40 Han Y, Yang J, Fang J, Zhou Y, Candi E, Wang J, et al. The secretion profile of mesenchymal stem cells and potential applications in treating human diseases. *Signal Transduct Target Ther* 2022;**7**:92.

41 Rivera-Cruz CM, Shearer JJ, Figueiredo Neto M, Figueiredo ML. The Immunomodulatory Effects of Mesenchymal Stem Cell Polarization within the Tumor Microenvironment Niche. *Stem Cells Int* 2017;**2017**:4015039.

42 Coomes SM, Wilke CA, Moore TA, Moore BB. Induction of TGF-beta 1, not regulatory T cells, impairs antiviral immunity in the lung following bone marrow transplant. *J Immunol* 2010;**184**:5130-40.

43 Liu L, Chiu PW, Lam PK, Poon CC, Lam CC, Ng EK, et al. Effect of local injection of mesenchymal stem cells on healing of sutured gastric perforation in an experimental model. *Br J Surg* 2015;**102**:e158-68.

44 Hinz B. The extracellular matrix and transforming growth factor-beta1: Tale of a strained relationship. *Matrix Biol* 2015;**47**:54-65.

45 Wu Y, Chen L, Scott PG, Tredget EE. Mesenchymal stem cells enhance wound healing through differentiation and angiogenesis. *Stem Cells* 2007;**25**:2648-59.

46 Madonna R, Delli Pizzi S, Tartaro A, De Caterina R. Transplantation of mesenchymal cells improves peripheral limb ischemia in diabetic rats. *Mol Biotechnol* 2014;**56**:438-48.

47 Khubutiya MS, Vagabov AV, Temnov AA, Sklifas AN. Paracrine mechanisms of proliferative, anti-apoptotic and anti-inflammatory effects of mesenchymal stromal cells in models of acute organ injury. *Cytotherapy* 2014;**16**:579-85.

48 Carmeliet P, Jain RK. Molecular mechanisms and clinical applications of angiogenesis. *Nature* 2011;**473**:298-307.

49 Khan S, Villalobos MA, Choron RL, Chang S, Brown SA, Carpenter JP, et al. Fibroblast growth factor and vascular endothelial growth factor play a critical role in endotheliogenesis from human adipose-derived stem cells. *J Vasc Surg* 2017;**65**:1483-92.

50 Lopatina T, Bruno S, Tetta C, Kalinina N, Porta M, Camussi G. Platelet-derived growth factor regulates the secretion of extracellular vesicles by adipose mesenchymal stem cells and enhances their angiogenic potential. *Cell Commun Signal* 2014;**12**:26.

51 Harrell CR, Djonov V, Volarevic V. The Cross-Talk between Mesenchymal Stem Cells and Immune Cells in Tissue Repair and Regeneration. *Int J Mol Sci* 2021;**22**.

52 Tao H, Han Z, Han ZC, Li Z. Proangiogenic Features of Mesenchymal Stem Cells and Their Therapeutic Applications. *Stem Cells Int* 2016;**2016**:1314709.

53 Louis SF, Zahradka P. Vascular smooth muscle cell motility: From migration to invasion. *Exp Clin Cardiol* 2010;**15**:e75-85.

54 Swijnenburg RJ, Schrepfer S, Govaert JA, Cao F, Ransohoff K, Sheikh AY, et al. Immunosuppressive therapy mitigates immunological rejection of human embryonic stem cell xenografts. *Proc Natl Acad Sci U S A* 2008;**105**:12991-6.

55 Rong Z, Wang M, Hu Z, Stradner M, Zhu S, Kong H, et al. An effective approach to prevent immune rejection of human ESC-derived allografts. *Cell Stem Cell* 2014;**14**:121-30.

56 Lezmi E, Benvenisty N. The Tumorigenic Potential of Human Pluripotent Stem Cells. *Stem Cells Transl Med* 2022;**11**:791-6.

APPENDICES

CLTI, critical limb-threatening ischemia; MSC, mesenchymal stem cells; E-MSCs, embryonic stem cell-derived mesenchymal stem cells; LDPI, laser Doppler perfusion imaging system; qPCR, quantitative polymerase chain reaction; TNF-α, tumor necrosis factor-alpha; IL, interleukin; TGF-β, transforming growth factor-beta; ANG, angiopoietins; FGF, fibroblast growth factor; VEGF, vascular endothelial growth factor; PDGF, platelet-derived growth factor; GAPDH, glyceraldehyde 3-phosphate dehydrogenase; IHC, immunohistochemistry; H&E, hematoxylin and eosin; MT, masson's trichrome; a-SMA, alpha-smooth muscle actin.

ABSTRACT IN KOREAN

중증 사지 허혈의 쥐 모델에서 중간엽 줄기 세포 치료의 효능 및 최소 유효 용량 평가

목적: 본 연구는 배아 줄기 세포로부터 유래한 중간엽 줄기세포 (E-MSCs)가 심각한 사지 위협 허혈 (CLTI)과 같은 허혈성 상태에서 조직 손상 완화 및 혈관신생 촉진의 치료 잠재력을 조사하는 것이다. 또한, 효과적인 치료 결과를 달성하기 위해 필요한 최적 용량을 결정하고자 하였다.

재료 및 방법: 85마리의 BALB/c 누드 마우스 (7주령, 암컷)를 사용하여 하지 허혈 모델을 확립하였다. 마우스는 각각 17마리씩 다섯 그룹으로 나누었다: 비허혈 (그룹 1, 무처리군), 생리식염수 처리 허혈 (그룹 2, 대조군), 저용량, 중간 용량, 고용량의 E-MSC 처리 허혈 (그룹 3-5). 효능과 최소 유효 용량은 회전막대 실험, 괴사 측정, 혈액 관류 비율 (혈류율), 조직학적 및 염증 및 혈관신생 사이토카인 분석을 통해 평가되었다.

결과: 레이저 도플러 관류 검사는 E-MSC 처리 그룹에서 혈류율이 대조군에 비해 유의하게 회복되었으며, 중간 용량의 E-MSC 처리 그룹이 가장 뚜렷한 개선을 보였다. E-MSC 처리 그룹에서는 시간이 지남에 따라 운동 기능이 향상되었지만, 그룹간 괴사 점수에는 유의한 차이가 없었다. 염증성 사이토카인(TNF-α, IL-1β, IL-6 및 TGF-β) 및 혈관신생 사이토카인(ANG-1, FGF, VEGF 및 PDGF)의 발현은 허혈 유도 그룹에서 증가하였다. E-MSC 처리 그룹에서는 그룹 2와 비교하여 초기 염증성 사이토카인의 발현이 감소한 반면, 혈관신생 사이토카인의 발현은 증가하였다. 그러나 E-MSC 용량에 따른 유의한 차이는 발견되지 않았다. 허혈 유도 그룹은 비허혈 그룹에 비해 근섬유 두께 및 수가 감소하고, 침윤된 염증 세포 및 콜라겐 섬유가 증가하였다. 시간이 지남에 따라 E-MSC 처리 그룹은 대조군에 비해 유사한 근섬유 두께를 보였으나, 근섬유 수가 증가하고 침윤된 염증 세포 및 콜라겐 섬유가 감소하였으며, 용량 의존적인 차이는 없었다.

결론: E-MSC는 하지 허혈 모델에서 혈류율을 개선하고 염증 및 혈관신생 사이토카인을 조절하였으나, 용량에 따른 차이는 유의하지 않았다. 이러한 세포는 조직복구에 필수적인 혈관신생 및 면역조절 효과를 나타내지만, 이들의 효능을 극대화하기 위한 최적의 용량을 결정하고, 임상적용을 위한 메커니즘을 명확히 이해하기 위해서는 추가 연구가 필요합니다.

핵심되는 말: 배아줄기세포유래 중간엽줄기세포, 혈관신생, 면역조절, 말초동맥질환, 중증사지허혈

PUBLICATION LIST

1 Kim DJ, Hahn HM, Youn YN, Lee JS, Lee IJ, Lim SH. Adipose Derived Stromal Vascular Fraction and Mesenchymal Stem Cells Improve Angiogenesis in a Rat Hindlimb Ischaemia Model. *Eur J Vasc Endovasc Surg* 2024;**67**:828-37.